Advances in Meshless Modeling of Material Damage.

J. Michael Owen[1]
[1]Lawrence Livermore National Laboratory, (mikeowen@llnl.gov)

Introduction: The work we present here is an extension of the SPH (Smoothed Particle Hydrodynamics) formalism for modeling material failure and fracture in [1], which was developed for modeling impacts and cratering on small solar system bodies. Our techniques have been benchmarked against a number of laboratory experiments, some of which are discussed below. In a separate presentation we discuss the application to modeling mega-cratering on the Martian moon Phobos.

(a) SPH

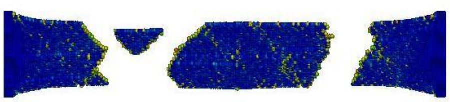

(b) ASPH

Figure 1: SPH vs. ASPH models of a steel rod undergoing tension, colored by damage.

ASPH: Adaptive Smoothed Particle Hydrodynamics (ASPH, see [3] & [4]) differs from SPH in the choice of sampling volume. SPH associates a scalar smoothing scale with each SPH point (usually denoted as h_i for point i), representing the resolution scale around that point. This scale is usually evolved inversely with the mass density in order to keep a roughly constant number of neighbor points within each sampling volume. This approximation breaks down however as the local point density begins to evolve anisotropically. ASPH replaces h_i with a symmetric tensor $H_i^{\alpha\beta}$, corresponding to a unique elliptical (2D) or ellipsoidal (3D) sampling volume for each ASPH point. $H_i^{\alpha\beta}$ is evolved such that each point keeps the same number of neighbors *in each direction* within its local sampling volume. This can be very important in avoiding numerical failure in materials undergoing stress, as demonstrated in Fig. 1. Here we model a steel rod being stretched in the horizontal direction – SPH's inability to preferentially increase the smoothing scale in that direction causes the SPH rod to preemptively fall apart numerically, while the ASPH model successfully follows the deformation of the material until it fractures at the points indicated by the damage model.

Damage modeling: We have augmented the damage models described in [1] (based on the statistical fragmentation theory of [2]) in a few important ways. First we have extended the concept of the damage to a tensor formalism ($D_i \rightarrow D_i^{\alpha\beta}$), which gives us directionality in the damage on each node. We have also developed a pair-wise limiter based on the gradient of the damage to determine when a given pair of ASPH nodes should apply damage to their interactions. Our changes are designed to focus the damage into evolving fractures and relieve strain on the bulk of material more effectively, avoiding a common failure mode where the computational damage becomes too wide-spread (the most extreme form of these problems result in all the material becoming damaged and turning into an undifferentiated dust). We have found these handful of extensions very helpful in demonstrating convergence of the models and successfully matching experiments.

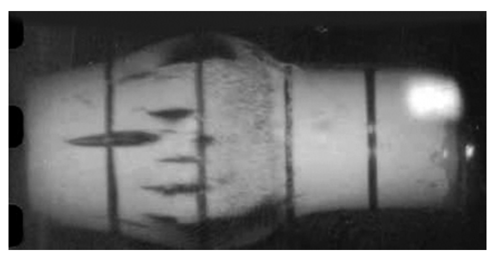

(a) Experiment

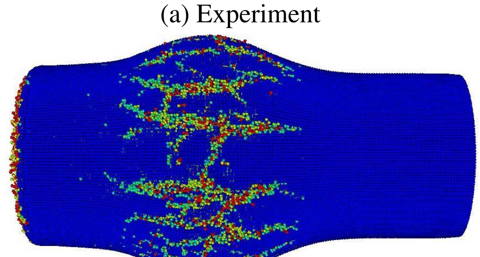

(b) Calculation (damage)

Figure 2: Simulated damage vs. the experimental photograph in the gas gun experiment.

Experimental comparisons: We have applied our modeling methodology to a series of laboratory experiments in order to test their validity. In one example [5] a steel tube (5cm long by 1.27cm diameter) is fitted to an anvil on a gas gun. Half the length of tube is filled with a plastic plug, while a similar plastic plug is fired into the open end of the tube at $\sim$ 2km/sec. When the projectile impacts the plug in the tube the two expand outward, fracturing the surrounding steel. Fig. 2 compares the experimental photograph to the simulated tube at 35 μsec. We have been able to successfully match quantities such as expansion velocities, fragment mass statistics, and fragment morphology in experiments such as this.

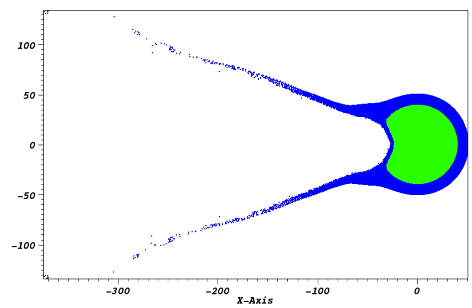

(a) Materials 0.1 sec after impact

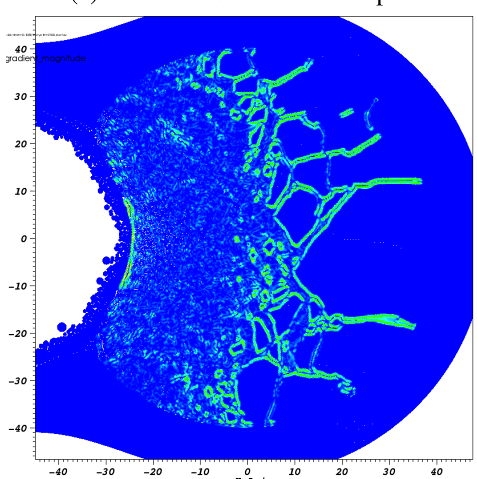

(b) Fractures in solid core

Figure 3: 2D simulations of 2m Al slug impacting a 50 m radius idealized asteroid.

Small body results: We are applying our methodology to understand the response of small solar system bodies to attempts to divert them, such as kinetic impactors or nuclear devices. Fig. 3 shows a 2D calculation of a 2×1m Al slug traveling at 12 km/sec impacting a 50 m radius granite asteroid, consisting of a 40 m radius solid core surrounded by 10m of strengthless regolith. Our model captures the disruption of the regolith layer, pulverization of the solid core near the impact point, and radiating fractures through the core outside of this fully damaged region. Fig. 3b plots our fracture detection switch used to decide which ASPH points should decouple, demonstrating the effectiveness of this switch at picking out the macroscopic fractures. It is important to capture these sorts of differences for our applications in order to predict both the deflection due to material which is ejected and results in deflection of the bulk material, as well as the fragmentation state of the remaining body. This has implications both for the practical considerations of deflection and/or disruption, as well as the fundamental science in determining the fate of interacting small solar system bodies and their resulting characteristics after numerous impacts such as these.

References

[1] W. Benz & E. Asphaug, (1995) Computers Phys. Comm., 87, 253-265.

[2] D. E. Grady & M. E. Kipp, (1980) Int. J. Rock Mech. Min. Sci. Geomech. Abstr., 17, 147-157.

[3] J. M. Owen, J. V. Villumsen, P. Shapiro, & H. Martell (1998), Ap. J. Supp., 116, 155-209.

[4] J. M. Owen, Proc. Fifth Int. SPHERIC Workshop (2010), Manchester, U.K., 297-307.

[5] T. J. Vogler, T. F. Thornhill, W. D. Reinhart, L. C. Chhabildas, D. E. Grady, L. T. Wilson, O. A. Hurricane, and A. Sunwoo, (2003) Int. J. Imp. Eng., 29, 735-746.

Acknowledgments: This work was performed under the auspices of the U.S. Department of Energy by Lawrence Livermore National Laboratory under Contract DE-AC52-07NA27344, and partially funded by the Laboratory Directed Research and Development Program at LLNL under tracking code 12-ERD-005.
LLNL-ABS-608234